

Vibration of nonlocal perforated nanobeams with general boundary conditions

Mohamed A. Eltahaer*^{1,2} and Norhan A. Mohamed^{3a}

¹ Mechanical Engineering Department, Faculty of Engineering, King Abdulaziz University, P.O. Box 80204, Jeddah, Saudi Arabia

² Mechanical Design and Production Department, Faculty of Engineering, Zagazig University, P.O. Box 44519, Zagazig, Egypt

³ Engineering Mathematics and Physics Department, Faculty of Engineering, Zagazig University, P.O. Box 44519, Zagazig, Egypt

(Received September 5, 2019, Revised November 13, 2019, Accepted November 20, 2019)

Abstract. This article presents a comprehensive model to investigate a free vibration and resonance frequencies of nanostructure perforated beam element as nano-resonator. Nano-scale size dependency of regular square perforated beam is considered by using nonlocal differential form of Eringen constitutive equation. Equivalent mass, inertia, bending and shear rigidities of perforated beam structure are developed. Kinematic displacement assumptions of both Timoshenko and Euler-Bernoulli are assumed to consider thick and thin beams, respectively. So, this model considers the effect of shear on natural frequencies of perforated nanobeams. Equations of motion for local and nonlocal elastic beam are derived. After that, analytical solutions of frequency equations are deduced as function of nonlocal and perforation parameters. The proposed model is validated and verified with previous works. Parametric studies are performed to illustrate the influence of a long-range atomic interaction, hole perforation size, number of rows of holes and boundary conditions on fundamental frequencies of perforated nanobeams. The proposed model is supportive in designing and production of nanobeam resonator used in nanoelectromechanical systems NEMS.

Keywords: resonance frequencies; free vibration; perforated nonlocal nanobeam; analytical solution; frequency equations

1. Introduction

Rapidly development of science and technology tends to new era of nanotechnology including engineering, chemical, medicine, electronics that will change the direction of our life. Nanobars, nanotubes, nanobeams and nanoplates are potential structural elements commonly used in nanotechnology. Especially, nanobeam structure is commonly used in many applications such as, atomic force microscope (Nagase *et al.* 2010), nanosensors (Joshi *et al.* 2011, Hashemi and Khaniki 2018), nanoswitches (Khadem *et al.* 2012), nano-probes (Barretta *et al.* 2018), nanoactuators and energy harvesters (Baroudi *et al.* 2018), rotational motors, nanotweezers (Li *et al.* 2018), and NEMS (Emam *et al.* 2018).

The size-dependent effects are often insignificant and neglected in macro-structures. However, many experimental works have been observed that nano/micro-scale structures have size dependent effects on their mechanical and physical properties. Accordingly, adopted non-classical continuum models such as micromorphic, micropolar, Cosserat, nonlocal, strain gradient and couple stress theories have been demonstrated to be reliable with atomic model at micro/nano-scale and include classical continuum mechanics at macroscale, Eltahaer *et al.* (2014). The nonlocal continuum theory, that developed by Eringen (1972, 1983 and 2002), has gained much popularity among

the researchers, because of its competence and easiness. The nonlocal theory is extracted from the lattice dynamics and phonon dispersions of atomic theory. Chen *et al.* (2004) demonstrated that the nonlocal continuum theories can be physically inferred from the molecular dynamics' perspective. The theory is proposed that the stress at a point in elastic continuum is a functional of strain field at every point in domain, Eltahaer *et al.* (2016). Huang (2012) presented uniform nonlocal kernel model to study the influences of the nonlocal long-range interactions on the vibration of a nanorod. Eltahaer *et al.* (2012, 2013a, b) inspected free vibration of both isotropic and functionally graded (FG) nanobeams by implemented differential form of nonlocal Eringen model and finite element method. A comprehensive review on the applicability of nonlocal nanobeam models in mechanical behaviors and responses is presented by Eltahaer *et al.* (2016). Akbaş (2016) studied forced vibration of a simple supported viscoelastic modified couple stress nanobeam by finite element method.

Apuzzo *et al.* (2017) presented stress-driven nonlocal integral model (SDM) to illustrate a vibrational behaviors of Bernoulli-Euler nanobeams. Shen *et al.* (2017) studied dynamics behaviors of silicon nanobeams with axial motion subjected to transverse and longitudinal loads considering nonlocal and surface effects. Kaghazian *et al.* (2017) studied free vibration of a piezoelectric nonlocal nanobeam by using based on Euler-Bernoulli beam theory. Mouffoki *et al.* (2017) presented effects of moisture and temperature on free vibration of FG nonlocal nanobeams resting on elastic foundation. Akbaş (2017a) exploited modified couple stress theory to study the free vibration of edge cracked of FG microscale beams. Eltahaer *et al.* (2018a) presented a modified porosity model to investigate the static and

*Corresponding author, Professor,

E-mail: meltahaer@kau.edu.sa; mmeltahaer@zu.edu.eg

^a Ph.D., E-mail: nalla@zu.edu.eg

dynamic behaviors of FG nonlocal porous nanobeams. Belmahi *et al.* (2018) investigated the vibration of single walled carbon nanotubes (SWCNTs) embedded in a polymeric matrix using nonlocal elasticity theories with account arbitrary boundary conditions effects. Akbaş (2017b, 2018a, b) studied forced vibration of FG microbeam with and without cracks by using modified couple stress theory and finite element method. Emam *et al.* (2018) studied postbuckling and free vibration behaviors of multilayer imperfect nonlocal nanobeams under a pre-stress load. Akbaş (2018c) illustrated the edge crack effect on static bending of cantilever FG nanobeam subjected to transversal point load. In framework of nonlocal strain gradient theory and the Euler-Bernoulli beam theory, Simsek (2019) studied mechanical behaviors and forced vibration of FG nanobeams and presented their closed-form solutions. Eltahaer *et al.* (2019a, b) explored the postbuckling and free vibration of perfect and imperfect CNTs by using energy equivalent method. Arani *et al.* (2019) studied wave propagation of FG nano-beams based on the nonlocal elasticity theory considering surface and flexoelectric effects. Hamed *et al.* (2019) investigated mechanical bending behaviors and vibrations of FG porous nonlocal nanobeams by using finite element method. Akbaş (2019) presented axially forced vibration response of cracked nonlocal nanorod under harmonic external dynamically load. Eltahaer *et al.* (2020b) studied the static buckling stability and mode-shapes of composite laminated beams under varying axial in-plane loads by using numerical differential quadrature method.

Perforation and etching of holes are frequently used in fabrication procedure of MEMS and NEMS, Luschi and Pieri (2014). Performance and behaviors of perforated beam structure are totally different than the fully beam structure. Jeong and Amabili (2006) studied vibration behaviors of perforated simply supported beams in contact with an ideal liquid and observed that natural frequencies are gradually reduced with an increase of the hole size. Mohite *et al.* (2008) offered a comprehensive model of squeeze-film damping in perforated 3-D MEMS structures. The influence of perforations on thermo-elastic damping and anchor losses in bulk plate resonators has been studied by Shao and Palaniapan (2008), Tu and Lee (2012). Sharma and Grover (2011) derived closed form expressions for the transverse vibrations of a homogenous isotropic thermo-elastic thin beam with voids. Luschi and Pieri (2012) presented compact analytical expressions for the equivalent bending stiffness of Euler-Bernoulli beam in the filled and perforated sections and used this model to compute the resonance frequencies of the perforated beam.

Luschi and Pieri (2014, 2016) developed closed expressions for the equivalent bending and shear stiffness of clamped-clamped beams with regular square perforations and determined their resonance frequencies. El-Sinawi *et al.* (2015) presented comprehensive approach to feedback control of membrane displacement in perforated RF-MEMS switches. Bourouina *et al.* (2016) investigated effects of thermal loads and nonlocal length scale on free vibration of simply-supported nanobeams perforated with periodic square holes. Zulkefli *et al.* (2018) investigated stresses of

perforated graphene NEM contact switches by 3D finite element simulation. In case of simply-supported boundary condition, Eltahaer *et al.* (2018b, c) studied bending, buckling and free vibration behaviors of perforated nonlocal nanobeams. Kerid *et al.* (2019) investigated the magnetic field, thermal loads and small scale effects on the dynamic behaviors of perforated nanobeams with periodic square networks. Abdalrahmaan *et al.* (2019) presented a unified mathematical model to investigate free and forced vibration responses of perforated thin and thick beams. Cortés *et al.* (2019) developed geometry simplification of open-cell porous materials for elastic deformation by using finite element analysis. Almitani *et al.* (2019) introduced a semi-analytical model capable of investigating the dynamic performance of perforated beam structure under free and forced conditions. Eltahaer *et al.* (2020a) investigated mechanical behaviors of piezoelectric nonlocal nanobeam with cutouts.

To the author's awareness, vibration behaviors of perforated thin/thick nanobeams including a size scale effect with generalized boundary conditions have not been studied. Consequently, this manuscript aims to fill this gap in the literature and present closed form and numerical solution of the frequency equations in case of generalized boundary conditions. This article is organized as follows: Section 2 portrays geometrical adaptation of perforated nanobeams. Mathematical models of thin and thick of perforated nanobeams modelled by nonlocal differential form of Eringen are also presented in Section 2. A closed form solutions and frequency equations for perforated nonlocal nanobeam with generalized boundary conditions are derived and illustrated in Section 3. Section 4 is devoted to validate a proposed model and present effects of length scale parameter, number of perforated holes, perforation size, shear effects, and boundary conditions on natural frequencies of perforated beams in nanoscale. Main observations, investigations and conclusions are briefed in Section 5.

2. Problem formulation

2.1 Geometrical modification

Perforated beam is generally fabricated by sacrificial etching through a pattern of holes. These holes are squared in shape arranged in grid pattern, that used commonly in MEMS and NEMS applications. Due to perforation process, a geometrical adaptation will be affected on mechanical and electrical behaviors of perforated structure. In perforated beam analysis, the modification in bending stiffness, shear stiffness, mass inertia, and rotary inertia parameters must be considered. So, the modified expressions for these parameters will be depicted in detail through the next paragraph.

The geometry of perforated nanobeam is shown in Fig. 1. As illustrated, the perforated beam has a length of L , width of w and thickness of h . A beam is perforated with a pattern of square holes, that has spatial period l_s and side $l_s - t_s$, and a number of hole-rows N along the section.

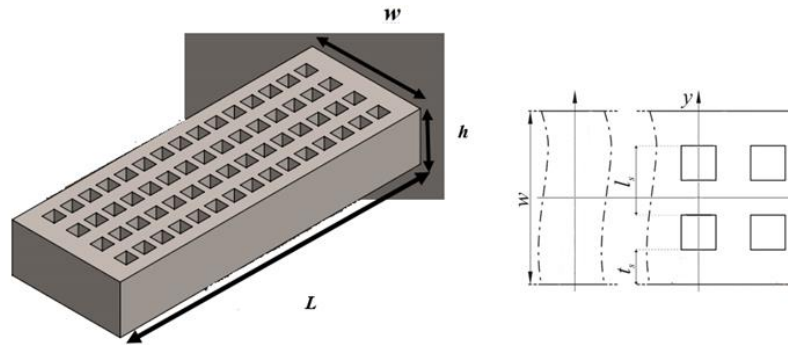


Fig. 1 A perforated beam with geometrical parameters

The filling ratio which is defined as the ratio of material thickness between two holes to the period length, can be formulated as

$$\alpha = \frac{t_s}{l_s} \quad 0 \leq \alpha \leq 1 \quad (1)$$

that means the beam is completely filled at filling ratio $\alpha = 1$, partially filling when $0 \leq \alpha \leq 1$, and completely perforated at $\alpha = 0$. From engineering view, the normal stress will be abridged in the parts between holes, which will be under-stressed with respect to the full beam case, and will be over-stressed in the remaining parts. By assuming that the total stress along the cross section is the same for both complete beam and perforated one and assuming a linear continuous stress distribution in the filled segments. Under this hypothesis, the equivalent bending stiffness can be depicted by Abdalrahmaan *et al.* (2019) as

$$(EI)_{eq} = EI \frac{\alpha(N+1)(N^2+2N+\alpha^2)}{(1-\alpha^2+\alpha^3)N^3+3\alpha N^2+(3+2\alpha-3\alpha^2+\alpha^3)\alpha^2 N+\alpha^3} \quad (2)$$

Considering the shear effect of perforated nanobeam, the shear stiffness will be modified as Eltaher *et al.* (2018b)

$$(GA)_{eq} = GA \frac{\alpha^3(N+1)}{2N} \quad (3)$$

It is noted that from Eq. (3), the shear stiffness is dependent on both filling ratio and number of holes. But, the filling ratio is more pronounced on the shear stiffness than the number of holes. The mass of the perforated beam per unit length can be modified as Luschi and Pieri (2014)

$$(\rho A)_{eq} = \rho A \frac{[1-N(\alpha-2)]\alpha}{N+\alpha} \quad (4)$$

The equivalent moment of inertia per unit length can be calculated by integrating over a strip of N square cells of length l_s , (Abdalrahmaan *et al.* 2019)

$$(\rho I)_{eq} = \rho I \frac{\alpha \left[\frac{(2-\alpha)N^3+3N^2}{-2(\alpha-3)(\alpha^2-\alpha+1)N+\alpha^2+1} \right]}{(N+\alpha)^3} \quad (5)$$

The equivalent moment of inertia per unit length can be calculated by integrating over a strip of N square cells of length l_s , (Abdalrahmaan *et al.* 2019).

2.2 Nonlocal constitutive equations

The basis of nonlocal elasticity assumed that the stress at a point is a functional of strain field at every point in body domain. The nonlocal constitutive equation can be depicted by Eltaher *et al.* (2016a, 2018a, b)

$$\sigma_{ij}(x) = \int_V \alpha(|x'-x|, \tau) t_{ij}(x') dx' \quad (6)$$

in which $t_{ij}(x')$ are the macroscopic stress tensor at point x and $\alpha(|x'-x|, \tau)$ is nonlocal modulus function that represents the effect of interatomic bonding. τ is a material length scale constant. The macroscopic stress tensor can be described as a function of material elasticity tensor (C) and strain (ε) by generalized Hooke's law as

$$t(x) = C(x):\varepsilon(x) \quad (7)$$

In 1983, Eringen (1983) proved that when nonlocal modulus described by a Green's function, the nonlocal constitutive relation can be reduced to the differential form as

$$[1 - (e_0 a)^2 \nabla^2] \sigma_{ij} = t_{ij} \quad (8)$$

where e_0 is a constant to match the reliable results by experiments, a is the internallength scale, and ∇^2 is the Laplacian operator. For one-dimensional nonlocal-nanobeam, nonlocal constitute relation (Eq. (18)) can be written as

$$\sigma_{xx} - \mu \frac{\partial^2 \sigma_{xx}}{\partial x^2} = E \varepsilon_{xx}; \quad [\mu = (e_0 a)^2] \quad (9a)$$

$$\sigma_{xz} - \mu \frac{\partial^2 \sigma_{xz}}{\partial x^2} = G \gamma_{xz} \quad (9b)$$

2.3 Governing equations of perforated nanobeams

2.3.1 Perforated Thin Nanobeam (PNEB)

In case of thin beam, kinematics assumptions of Euler-

Bernoulli theory can be applied as follows

$$u(x, z, t) = u_0(x, t) - z \frac{\partial w_0(x, t)}{\partial x} \quad (10a)$$

$$w(x, z, t) = w_0(x, t) \quad (10b)$$

in which u is the inplane and w is the out of plane displacements at any generic point. u_0 and w_0 are displacements along the neutral axis. Since, the axial displacement along neutral axis is very small comparable with transverse displacement and rotation, so it can be neglected. The strain can be defined by

$$\begin{aligned} \varepsilon_{xx} &= \frac{\partial u(x, z, t)}{\partial x} \\ &= \frac{\partial u_0(x, t)}{\partial x} - z \frac{\partial^2 w_0(x, t)}{\partial x^2} = \varepsilon_{xx}^0 + z k_0 \end{aligned} \quad (11)$$

So, equation of motion of thin beam can be depicted by, Eltahir *et al.* (2013a)

$$\frac{\partial N_R}{\partial x} + f(x, t) = m_0 \frac{\partial^2 u}{\partial t^2} \quad (12a)$$

$$\begin{aligned} \frac{\partial^2 M_R}{\partial x^2} + q(x, t) - \frac{\partial}{\partial x} \left(N_b \frac{\partial w}{\partial x} \right) \\ = m_0 \frac{\partial^2 w}{\partial t^2} - m_2 \frac{\partial^4 w}{\partial x^2 \partial t^2} \end{aligned} \quad (12b)$$

in which N_R and M_R are axial force and bending moment resultants. f and q are the axial and transverse vertical distributed loads. N_b is the axial compressive force. The translated mass inertia and rotary inertia of perforated beam are described by

$$m_0 = \int_A \rho dA = (\rho A)_{eq} \quad (13a)$$

$$m_2 = \rho \int_A \frac{h}{l_s} (x^2 + y^2) dx dy = (\rho I)_{eq} \quad (13b)$$

The axial force and bending moment resultants can be described as following

$$N_R = \int_A E \varepsilon_{xx} dA = (EA)_{eq} \frac{\partial u_0}{\partial x} \quad (14a)$$

$$M_R = \int_A z E \varepsilon_{xx} dA = -(EI)_{eq} \frac{\partial^2 w_0}{\partial x^2} \quad (14b)$$

where E is the Young modulus and I is the area moment of cross-section. By substituting Eq. (14) into Eq. (12), the equation of motion of thin beam in terms of displacements can be derived as

$$(EA)_{eq} \frac{\partial^2 u_0}{\partial x^2} + f(x, t) = m_0 \frac{\partial^2 u_0}{\partial t^2} \quad (15a)$$

$$\begin{aligned} (EI)_{eq} \frac{\partial^4 w_0}{\partial x^4} + q(x, t) - \frac{\partial}{\partial x} \left(N_b \frac{\partial w_0}{\partial x} \right) \\ = m_0 \frac{\partial^2 w_0}{\partial t^2} - m_2 \frac{\partial^4 w_0}{\partial x^2 \partial t^2} \end{aligned} \quad (15b)$$

Based on the nonlocal constitutive relations Eq. (9), the nonlocal force and moment resultants can be derived as

$$N_R - \mu \frac{\partial^2 N_R}{\partial x^2} = (EA)_{eq} \frac{\partial u_0}{\partial x} \quad (16a)$$

$$M_R - \mu \frac{\partial^2 M_R}{\partial x^2} = -(EI)_{eq} \frac{\partial^2 w_0}{\partial x^2} \quad (16b)$$

that can be handle as follows

$$N_R = (EA)_{eq} \frac{\partial u_0}{\partial x} + \mu \left(m_0 \frac{\partial^3 u_0}{\partial x \partial t^2} - \frac{\partial f}{\partial x} \right) \quad (17a)$$

$$\begin{aligned} M_R = -(EI)_{eq} \frac{\partial^2 w_0}{\partial x^2} \\ - \mu \left[N_b \frac{\partial^2 w_0}{\partial x^2} - q + m_0 \frac{\partial^2 w_0}{\partial t^2} - m_2 \frac{\partial^4 w_0}{\partial x^2 \partial t^2} \right] \end{aligned} \quad (17b)$$

Substituting Eq. (16) into Eq. (12), results the following equations of motion as

$$\begin{aligned} (EA)_{eq} \frac{\partial^2 u_0}{\partial x^2} + \left[1 - \mu \frac{\partial^2}{\partial x^2} \right] f \\ = \left[1 - \mu \frac{\partial^2}{\partial x^2} \right] m_0 \frac{\partial^2 u_0}{\partial t^2} \end{aligned} \quad (18a)$$

$$\begin{aligned} -(EI)_{eq} \frac{\partial^4 w_0}{\partial x^4} + \left[1 - \mu \frac{\partial^2}{\partial x^2} \right] \left[q - N_b \frac{\partial^2 w_0}{\partial x^2} \right] \\ = \left[1 - \mu \frac{\partial^2}{\partial x^2} \right] \left[m_0 \frac{\partial^2 w_0}{\partial t^2} - m_2 \frac{\partial^4 w_0}{\partial x^2 \partial t^2} \right] \end{aligned} \quad (18b)$$

According to the following nonlocal natural boundary conditions at the beam boundaries $x = 0, L$

$$\bar{N} - (EA)_{eq} \frac{\partial u_0}{\partial x} - \mu \left(m_0 \frac{\partial^3 u_0}{\partial x \partial t^2} - \frac{\partial f}{\partial x} \right) = 0 \quad (19a)$$

$$\begin{aligned} \bar{M} + (EI)_{eq} \frac{\partial^2 w_0}{\partial x^2} - \mu \left[N_b \frac{\partial^2 w_0}{\partial x^2} - q \right. \\ \left. + m_0 \frac{\partial^2 w_0}{\partial t^2} - m_2 \frac{\partial^4 w_0}{\partial x^2 \partial t^2} \right] = 0 \end{aligned} \quad (19b)$$

$$\begin{aligned} \bar{V} + (EA)_{eq} \frac{\partial^3 w_0}{\partial x^3} - \mu \left[N_b \frac{\partial^3 w_0}{\partial x^3} - \frac{\partial q}{\partial x} \right. \\ \left. + m_0 \frac{\partial^3 w_0}{\partial x \partial t^2} - m_2 \frac{\partial^5 w_0}{\partial x^3 \partial t^2} \right] - m_2 \frac{\partial^3 w_0}{\partial x \partial t^2} = 0 \end{aligned} \quad (19c)$$

where \bar{N} , \bar{M} and \bar{V} represented the generalized forces.

2.3.2 Perforated Thick Nanobeam (PNTB)

As the thickness to length of the beam reduces to less than 20, the shear effect should be considered and kinematics assumptions of Timoshenko beam theory can be applied as following

$$u(x, z, t) = u_0(x, t) + z\phi(x, t) \tag{20a}$$

$$w(x, z, t) = w_0(x, t) \tag{20b}$$

in which ϕ is the rotation of the cross section. Based on Eq. (20), the nonzero strains are

$$\epsilon_{xx} = \frac{\partial u(x, z, t)}{\partial x} = \frac{\partial u_0(x, t)}{\partial x} + z \frac{\partial \phi(x, t)}{\partial x} \tag{21a}$$

$$\begin{aligned} \epsilon_{xz} &= \frac{1}{2} \left[\frac{\partial u(x, z, t)}{\partial z} + \frac{\partial w(x, z, t)}{\partial x} \right] \\ &= \frac{1}{2} \left[\phi(x, t) + \frac{\partial w_0(x, t)}{\partial x} \right] = \frac{1}{2} \gamma_{xz} \end{aligned} \tag{21b}$$

According to Eq. (21b), the shear is constant through the beam thickness, which is impractical. To compensate the error due to constant shear, the shear correction factor is proposed. The governing equations of Timoshenko beam can be represented by

$$\frac{\partial N}{\partial x} + f(x, t) = m_0 \frac{\partial^2 u_0}{\partial t^2} \tag{22a}$$

$$\frac{\partial Q}{\partial x} + q(x, t) - \frac{\partial}{\partial x} \left(N_b \frac{\partial w_0}{\partial x} \right) = m_0 \frac{\partial^2 w_0}{\partial t^2} \tag{22b}$$

$$\frac{\partial M}{\partial x} - Q = m_2 \frac{\partial^2 \phi}{\partial t^2} \tag{22c}$$

where Q is the shear force resultant, which can be calculated by

$$\begin{aligned} Q &= k_s \int_A \sigma_{xz} dA = k_s GA \gamma_{xz} \\ &= k_s GA \left[\phi(x, t) + \frac{\partial w_0(x, t)}{\partial x} \right] \end{aligned} \tag{23}$$

in which k_s is a shear correction factor, G is a shear modulus. Equations of motion can be prescribed in terms of displacement field by

$$(EA)_{eq} \frac{\partial^2 u_0}{\partial x^2} + f(x, t) = m_0 \frac{\partial^2 u_0}{\partial t^2} \tag{24a}$$

$$\begin{aligned} k_s(GA)_{eq} \left[\frac{\partial \phi}{\partial x} + \frac{\partial^2 w_0}{\partial x^2} \right] + q(x, t) - \frac{\partial}{\partial x} \left(N_b \frac{\partial w_0}{\partial x} \right) \\ = m_0 \frac{\partial^2 w_0}{\partial t^2} \end{aligned} \tag{24b}$$

$$(EI)_{eq} \frac{\partial^2 \phi}{\partial x^2} - k_s(GA)_{eq} \left[\phi(x, t) + \frac{\partial w_0}{\partial x} \right] = m_2 \frac{\partial^2 \phi}{\partial t^2} \tag{24c}$$

In case of nonlocal perforated thick nanobeam, the nonlocal resultant forces of Timoshenko beam can be deduced by handling Eq. (9) and Eq. (21) as

$$N - \mu \frac{\partial^2 N}{\partial x^2} = (EA)_{eq} \frac{\partial u_0}{\partial x} \tag{25a}$$

$$M - \mu \frac{\partial^2 M}{\partial x^2} = (EI)_{eq} \frac{\partial \phi}{\partial x} \tag{25b}$$

$$Q - \mu \frac{\partial^2 Q}{\partial x^2} = (GA)_{eq} k_s \gamma_{xz} = (GA)_{eq} k_s \left[\phi + \frac{\partial w_0}{\partial x} \right] \tag{25c}$$

which can be represented in terms of displacements as

$$N = (EA)_{eq} \frac{\partial u_0}{\partial x} + \mu \left[m_0 \frac{\partial^3 u_0}{\partial x \partial t^2} - \frac{\partial f}{\partial x} \right] \tag{26a}$$

$$\begin{aligned} M = (EI)_{eq} \frac{\partial \phi}{\partial x} + \mu \left[N_b \frac{\partial^2 w_0}{\partial x^2} - q + m_0 \frac{\partial^2 w_0}{\partial t^2} \right. \\ \left. - m_2 \frac{\partial^3 \phi}{\partial x \partial t^2} \right] \end{aligned} \tag{26b}$$

$$\begin{aligned} Q = (GA)_{eq} k_s \left[\phi + \frac{\partial w_0}{\partial x} \right] \\ + \mu \left[N_b \frac{\partial^3 w_0}{\partial x^3} - \frac{\partial q}{\partial x} + m_0 \frac{\partial^3 w_0}{\partial x \partial t^2} \right] \end{aligned} \tag{26c}$$

Hence, equations of motion of PNTB in terms of displacements can be represented

$$\begin{aligned} (EA)_{eq} \frac{\partial^2 u_0}{\partial x^2} + \left[1 - \mu \frac{\partial^2}{\partial x^2} \right] f \\ = \left[1 - \mu \frac{\partial^2}{\partial x^2} \right] m_0 \frac{\partial^2 u_0}{\partial t^2} \end{aligned} \tag{27a}$$

$$\begin{aligned} (GA)_{eq} k_s \left[\frac{\partial \phi}{\partial x} + \frac{\partial^2 w_0}{\partial x^2} \right] \\ + \left[1 - \mu \frac{\partial^2}{\partial x^2} \right] \left[q(x, t) - N_b \frac{\partial^2 w_0}{\partial x^2} \right] \\ = \left[1 - \mu \frac{\partial^2}{\partial x^2} \right] m_0 \frac{\partial^2 w_0}{\partial t^2} \end{aligned} \tag{27b}$$

$$\begin{aligned} (EI)_{eq} \frac{\partial^2 \phi}{\partial x^2} - (GA)_{eq} k_s \left[\phi + \frac{\partial w_0}{\partial x} \right] \\ = \left[1 - \mu \frac{\partial^2}{\partial x^2} \right] m_2 \frac{\partial^2 \phi}{\partial t^2} \end{aligned} \tag{27c}$$

and their boundary conditions at the beam boundaries are

$$\bar{N} - \left\{ (EA)_{eq} \frac{\partial u_0}{\partial x} + \mu \left[m_0 \frac{\partial^3 u_0}{\partial x \partial t^2} - \frac{\partial f}{\partial x} \right] \right\} = 0 \tag{28a}$$

$$\begin{aligned} \bar{M} - \left\{ (EI)_{eq} \frac{\partial \phi}{\partial x} + \mu \left[N_b \frac{\partial^2 w_0}{\partial x^2} - q \right. \right. \\ \left. \left. + m_0 \frac{\partial^2 w_0}{\partial t^2} + m_2 \frac{\partial^3 \phi}{\partial x \partial t^2} \right] \right\} = 0 \end{aligned} \tag{28b}$$

$$\bar{V} - \left\{ (GA)_{eq} k_s \left[\phi + \frac{\partial w_0}{\partial x} \right] - N_b \frac{\partial w_0}{\partial x} + \mu \left[N_b \frac{\partial^3 w_0}{\partial x^3} - \frac{\partial q}{\partial x} + m_0 \frac{\partial^3 w_0}{\partial x \partial t^2} \right] \right\} = 0 \quad (28c)$$

3. Analytical solution

The natural frequencies and vibrational behavior of perforated nanobeam are solved analytically by separation of variable method. By setting the applied forces f and q to zero, and assuming the nanobeam under constant axial compressive load $N_b = \text{const}$. Since, the most significant frequencies of beam are the out of plane frequencies (transversal vibration), so that, the in-plane frequencies can be neglected with respect to out of plane frequencies.

3.1 Frequency equations of PNEB

In case of free vibration, it can be assumed that periodic solutions of motion equation (Eq. (18b)) have the form $w_0(x, t) = W_0(x)e^{i\omega t}$, in which $W_0(x)$ is the spatial mode shape (eigenvector) and ω is the natural frequency (eigenvalue) of vibration. By substituting of periodic functions into Eq. (18b), obtains

$$\begin{aligned} & \left[-(EI)_{eq} \frac{\partial^4}{\partial x^4} (W_0(x)e^{i\omega t}) \right] \\ & - \left[1 - \mu \frac{\partial^2}{\partial x^2} \right] \left[N_b \frac{\partial^2}{\partial x^2} (W_0(x)e^{i\omega t}) \right] \\ = & \left[1 - \mu \frac{\partial^2}{\partial x^2} \right] \left[m_0 \frac{\partial^2}{\partial t^2} (W_0(x)e^{i\omega t}) \right] \\ & - m_2 \frac{\partial^4}{\partial x^2 \partial t^2} (W_0(x)e^{i\omega t}) \end{aligned} \quad (29a)$$

Eq. (28a) can be simplified to

$$A W_0^{IV} + B W_0'' - C W_0(x) = 0 \quad (29b)$$

in which contact parameters are $A = [(EI)_{eq} - \mu N_b - \mu \omega^2 m_2]$, $B = [N_b + \omega^2 m_2 + \mu \omega^2 m_0]$, and $C = \omega^2 m_0$.

The general solution of Eq. (28) can be described as

$$W_0(x) = c_1 \sin(\alpha x) + c_2 \cos(\alpha x) + c_3 \sinh(\beta x) + c_4 \cosh(\beta x) \quad (30)$$

where, $\alpha^2 = \frac{1}{2A} (B + \sqrt{B^2 + 4AC})$ and $\beta^2 = \frac{1}{2A} (-B + \sqrt{B^2 + 4AC})$.

The slope can be computed by using Eq. (29a)

$$\frac{dW_0}{dx}(x) = \alpha(c_1 \cos(\alpha x) - c_2 \sin(\alpha x)) + \beta(c_3 \cosh(\beta x) + c_4 \sinh(\beta x)) \quad (31)$$

By substituting periodic solution into Eqs. (19b) and (19c), the stress resultants can be calculated b

$$M = [-AW_0'' - \mu CW_0]e^{i\omega t}, \quad (32)$$

$$V = [-A1W_0'' - B1W_0']e^{i\omega t} \quad (33)$$

where, $A1 = [(EA)_{eq} - \mu N_b - \mu \omega^2 m_2]$ and $B1 = [\omega^2 m_2 + \mu \omega^2 m_0]$.

3.1.1 Simply supported BCs

The simply supported boundary conditions at the beam boundaries $x = 0, L$ are specified by $W_0 = 0$ and $M = 0$ (Eq. (31)). Since, the nonlocal bending moment is dependent on both displacement and curvature. By applying the following conditions:- $W_0(x = 0) = W_0''(x = 0) = 0$ and $W_0(x = L) = W_0''(x = L) = 0$, to the general solution of Eq. (29), results in $c_2 = c_4 = 0$, and

$$c_1 \sin(\alpha L) + c_3 \sinh(\beta L) = 0 \quad (34a)$$

$$\begin{aligned} & c_1 [A\alpha^2 - C\mu] \sin(\alpha L) \\ & - c_3 [A\beta^2 + C\mu] \sinh(\beta L) = 0 \end{aligned} \quad (34b)$$

By solving the two equations of (31) simultaneously, yields $\sin(\alpha L) = 0$ or $\alpha_n = \frac{n\pi}{L}$, hence the closed form solution of natural frequencies can be determined by

$$\omega_n = \left(\frac{n\pi}{L} \right) \sqrt{\frac{(EI)_{eq} (n\pi/L)^2 - [1 - \mu (n\pi/L)^2] N_b}{[m_0 + m_2 (n\pi/L)^2] [1 + \mu (n\pi/L)^2]}} \quad (35)$$

3.1.2 Clamped BCs

In this case, the boundary condition at the beam boundaries $x = 0, L$ are

$$W_0 = 0, \quad W_0' = \frac{dw}{dx} = 0. \quad (36)$$

By applying these boundary conditions to Eqs. (29) and (30), then eliminating the coefficients c_3 and c_4 , yields in the following equations

$$\begin{cases} \sin(\alpha L) - \frac{\alpha}{\beta} \sinh(\beta L) & \cos(\alpha L) - \cosh(\beta L) \\ \alpha \cos(\alpha L) - \alpha \cosh(\beta L) & -(\alpha \sin(\alpha L) + \beta \sinh(\beta L)) \end{cases} \begin{cases} c_1 \\ c_2 \end{cases} = \{0\} \quad (37)$$

For nonzero deflection W_0 , the determinant of the coefficient matrix of the above equations must be zero

$$\begin{aligned} |K| = & 2 \times \alpha \times \beta - \alpha^2 \times \sin(\alpha L) \times \sinh(\beta L) \\ & + \beta^2 \times \sin(\alpha L) \times \sinh(\beta L) \\ & - 2 \times \alpha \times \beta \times \cos(\alpha L) \times \cosh(\beta L) = 0 \end{aligned} \quad (38)$$

with α and β from in the above determinant and solve it numerically to get the natural frequency ω .

3.1.3 Cantilever BCs

For this case, boundary conditions are

$$\begin{aligned} & \text{at } x = 0; \quad W_0 = 0, \quad \frac{dw}{dx} = 0 \\ & \& \text{at } x = L; \quad M = V = 0 \end{aligned} \quad (39)$$

Substitute with these conditions into Eq. (29), leads to the following equations

$$\begin{bmatrix} 0 & 1 & 0 & 1 \\ \alpha & 0 & \beta & 0 \\ (A\alpha^2 - C\mu)\sin(\alpha L) & (A\alpha^2 - C\mu)\cos(\alpha L) & -(A\beta^2 - C\mu)\sinh(\beta L) & -(C\mu - A\beta^2)\cosh(\beta L) \\ D1 & D2 & D3 & D4 \end{bmatrix} \begin{Bmatrix} c_1 \\ c_2 \\ c_3 \\ c_4 \end{Bmatrix} = \{0\} \quad (40)$$

Where

$$\begin{aligned} D1 &= A1\alpha^2\sin(\alpha L) - B\mu\alpha\cos(\alpha L), \\ D2 &= -[A1\alpha^2\cos(\alpha L) + B\mu\alpha\sin(\alpha L)], \\ D3 &= -[A1\beta^2\sinh(\beta L) + B\mu\beta\cosh(\beta L)], \\ D4 &= -[A1\beta^2\cosh(\beta L) + B\mu\beta\sinh(\beta L)]. \end{aligned}$$

For nonzero deflection W_0 , setting the determinant of the coefficient matrix of the above equations to zero, yields

$$\begin{aligned} |K| &= A \times B \times \mu \times \alpha \times \beta^3 - A \times B \times \mu \times \alpha^3 \times \beta \\ &+ 2 \times B \times C \times \mu^2 \times \alpha \times \beta \\ &- A1 \times C \times \mu \times \alpha^3 \times \cos(\alpha L) \sinh(\beta L) \\ &+ A1 \times C \times \mu \times \beta^3 \times \cosh(\beta L) \sin(\alpha L) \\ &- B \times C \times \mu^2 \times \alpha^2 \sin(\alpha L) \sinh(\beta L) \\ &+ B \times C \times \mu^2 \times \beta^2 \sin(\alpha L) \sinh(\beta L) \\ &- 2A \times B \times \mu \times \alpha^2 \times \beta^2 \times \sin(\alpha L) \sinh(\beta L) \\ &- A \times B \times \mu \times \alpha \times \beta^3 \cos(\alpha L) \cosh(\beta L) \\ &+ A \times B \times \mu \times \alpha^3 \times \beta \cos(\alpha L) \cosh(\beta L) \\ &- 2B \times C \times \mu^2 \times \alpha \times \beta \cos(\alpha L) \cosh(\beta L) \\ &- A1 \times C \times \mu \times \alpha \times \beta^2 \cos(\alpha L) \sinh(\beta L) \\ &+ A1 \times C \times \mu \times \alpha^2 \times \beta \sin(\alpha L) \cosh(\beta L) = 0 \end{aligned} \quad (41)$$

By substituting α and β in the above determinant, and solving it numerically to get the natural frequency ω .

3.1.4 Propped BCs

The boundary condition in the case of propped beam are

$$\begin{aligned} \text{at } x = 0; \quad W_0 = 0, \quad \frac{dw}{dx} = 0 \\ \& \text{ at } x = L; \quad W_0 = M = 0. \end{aligned} \quad (42)$$

Substitute with these conditions to Eq. (29), leads to the following relations

$$\begin{bmatrix} 0 & 1 & 0 & 1 \\ \alpha & 0 & \beta & 0 \\ \sin(\alpha L) & \cos(\alpha L) & \sinh(\beta L) & \cosh(\beta L) \\ (A\alpha^2 - C\mu)\sin(\alpha L) & (A\alpha^2 - C\mu)\cos(\alpha L) & -(A\beta^2 + C\mu)\sinh(\beta L) & -(A\beta^2 + C\mu)\cosh(\beta L) \end{bmatrix} \begin{Bmatrix} c_1 \\ c_2 \\ c_3 \\ c_4 \end{Bmatrix} = \{0\} \quad (43)$$

By setting the determinant of the coefficient matrix of the above equations to zero, yields in

$$\begin{aligned} |K| &= A(\alpha^2 + \beta^2) \\ &\times (\alpha\cos(\alpha L)\sinh(\beta L) - \beta\sin(\alpha L)\cosh(\beta L)) = 0 \\ \text{Since } A(\alpha^2 + \beta^2) &\neq 0, \text{ so:} \\ &(\alpha\cos(\alpha L)\sinh(\beta L) - \beta\sin(\alpha L)\cosh(\beta L)) = 0 \\ \text{and, } \alpha \times \tanh(\beta L) &= \beta \times \tan(\alpha L). \end{aligned}$$

Substitute with α and β into Eq. (41) and solve it numerically to get the natural frequency ω .

3.2 Frequency equations of PNTB

In case of thick nanobeam, assuming periodic solutions for both deflection $[w_0(x, t) = W_0(x)e^{i\omega t}]$ and rotation $[\phi(x, t) = \Phi(x)e^{i\omega t}]$. By substituting these assumptions into equations of motion of NTB (Eqs. (26b) and (26c), results

$$\begin{aligned} \frac{N_b}{(GA)_{eq}k_s} \mu W_0^{IV} + \left[1 - \frac{N_b}{(GA)_{eq}k_s} - \frac{\mu\omega^2 m_0}{GAk_s} \right] W_0'' \\ + \frac{\omega^2 m_0}{(GA)_{eq}k_s} W_0 + \Phi'' = 0 \end{aligned} \quad (44a)$$

$$\begin{aligned} [(EI)_{eq} - \mu\omega^2 m_2] \Phi'' \\ + [\mu\omega^2 m_2 - (GA)_{eq}k_s] \Phi - (GA)_{eq}k_s W_0' = 0 \end{aligned} \quad (44b)$$

By manipulating Eqs. (42a) and (42b), the transverse displacement variable can be represented by

$$\begin{aligned} \left[((EI)_{eq} - \mu\omega^2 m_2) \frac{\mu N_b}{GAk_s} \right] W_0^{VI} \\ + \left[((EI)_{eq} - \mu\omega^2 m_2) \left(1 - \frac{N_b}{(GA)_{eq}k_s} - \frac{\mu\omega^2 m_0}{(GA)_{eq}k_s} \right) \right. \\ + \left. \frac{\mu N_b}{(GA)_{eq}k_s} (\omega^2 m_2 - (GA)_{eq}k_s) \right] W_0^{IV} \\ + \left[(\omega^2 m_2 - (GA)_{eq}k_s) \left(1 - \frac{N_b}{(GA)_{eq}k_s} - \frac{\mu\omega^2 m_0}{(GA)_{eq}k_s} \right) \right. \\ + \left. \frac{\omega^2 m_0}{(GA)_{eq}k_s} ((EI)_{eq} - \mu\omega^2 m_2) \right] W_0'' \\ + \frac{\omega^2 m_0}{(GA)_{eq}k_s} (\omega^2 m_2 - (GA)_{eq}k_s) W_0 = 0 \end{aligned} \quad (45)$$

It is observed that, the six-order differential term is dependent on the axial force N_b . By neglecting the effect of the axial load, Eq. (43) can be reduced to

$$A_T W_0^{IV} + B_T W_0'' - C_T W_0 = 0 \quad (46)$$

in which

$$A_T = \left[((EI)_{eq} - \mu\omega^2 m_2) \left(1 - \frac{\mu\omega^2 m_0}{GAk_s} \right) \right] \quad (47a)$$

$$B_T = \left[\omega^2 m_0 \left(\frac{(EI)_{eq}}{(GA)_{eq} k_s} + \mu \right) + \omega^2 m_2 \left(1 - 2 \frac{\mu \omega^2 m_0}{(GA)_{eq} k_s} \right) \right] \quad (47b)$$

$$C_T = \omega^2 m_0 \left(1 - \frac{\omega^2 m_2}{(GA)_{eq} k_s} \right) \quad (47c)$$

The general solution of Eq. (44) can be presented by

$$W_0(x) = c_1 \sin(\alpha_T x) + c_2 \cos(\alpha_T x) + c_3 \sinh(\beta_T x) + c_4 \cosh(\beta_T x) \quad (48)$$

where, $\alpha_T^2 = \frac{1}{2A_T} (B_T + \sqrt{B_T^2 + 4A_T C})$ and $\beta_T^2 = \frac{1}{2A_T} (-B_T + \sqrt{B_T^2 + 4A_T C})$.

In case of $q = 0$ and $N_b = 0$, the rotation variable ϕ can be computed by

$$\phi = S_{11} \frac{\partial^3 W}{\partial x^3} + S_{22} \frac{\partial W}{\partial x} \quad (49)$$

where

$$S_{11} = \left[\frac{-(EI)_{eq} + \mu \omega^2 m_2}{(GA)_{eq} k_s - \omega^2 m_2} \right] \left[1 - \frac{\mu \omega^2 m_0}{(GA)_{eq} k_s} \right] \quad (50a)$$

$$S_{22} = \left[\frac{-(GA)_{eq} k_s}{(GA)_{eq} k_s - \omega^2 m_2} \right] \left[1 - \frac{\omega^2 m_0 (\mu \omega^2 m_2 - (EI)_{eq})}{((GA)_{eq} k_s)^2} \right] \quad (50b)$$

And, stress resultants can be computed by

$$M = -[EI - \mu \omega^2 m_2] \left(1 - \frac{\mu \omega^2 m_0}{GA k_s} \right) \frac{d^2 W}{dx^2} = -A \frac{d^2 W}{dx^2} \quad (51)$$

$$V = (GA)_{eq} k_s S_{11} \frac{\partial^3 W}{\partial x^3} + [(GA)_{eq} k_s S_{22} + (GA)_{eq} k_s - \mu \omega^2 m_0] \frac{\partial W}{\partial x} \quad (52)$$

3.2.1 Simply supported BCs

In case of simply supported beam, applying the boundary conditions $W_0 = 0$ and $M = 0$ at the beam boundaries $x = 0, L$, the frequency equation of NTB can be presented by

$$\omega_n = \left(\frac{n\pi}{L} \right)^2 \sqrt{\frac{(EI)_{eq}}{\left\{ \left[1 + \left(\frac{n\pi}{L} \right)^2 Ks \right] m_0 + \left(\frac{n\pi}{L} \right)^2 m_2 \right\} \left[1 + \left(\frac{n\pi}{L} \right)^2 \mu \right]}}$$

where $Ks = \frac{(EI)_{eq}}{(GA)_{eq}}$

in which Ks is the influence of shear deformation on the natural frequency. The condition $Ks = 0$ corresponds to the absence of the shear effect.

3.2.2 Clamped BCs

The boundary condition for clamped beam at the boundaries $x = 0, L$ are $W_0 = 0$, and $\phi = 0$. By applying these boundary conditions in Eqs. (46) and (47) then eliminating the coefficients c_3 and c_4 , yields the following equations

$$\begin{bmatrix} D1 & D2 \\ D3 & D4 \end{bmatrix} \begin{Bmatrix} c_1 \\ c_2 \end{Bmatrix} = \{0\} \quad (53)$$

where

$$D1 = \sin(\alpha_T L) - \frac{(-\alpha_T^3 S_{11} + \alpha_T S_{22})}{(\beta_T^3 S_{11} + \beta_T S_{22})} \sinh(\beta_T L)$$

$$D2 = \cos(\alpha_T L) - \cosh(\beta_T L)$$

$$D3 = (-\alpha_T^3 S_{11} + \alpha_T S_{22}) \cos(\alpha_T L)$$

$$- \frac{(-\alpha_T^3 S_{11} + \alpha_T S_{22})}{(\beta_T^3 S_{11} + \beta_T S_{22})}$$

$$\times (\beta_T^3 S_{11} + \beta_T S_{22}) \cosh(\beta_T L)$$

$$D4 = -((-\alpha_T^3 S_{11} + \alpha_T S_{22}) \sin(\alpha_T L))$$

$$+ (\beta_T^3 S_{11} + \beta_T S_{22}) \sinh(\beta_T L)$$

For nonzero deflection W_0 , the determinant of the coefficient matrix of the above equations must to be zero. Hence

$$\begin{aligned} & [S_{11}^2 (\beta_T^6 - \alpha_T^6) + 2 \times S_{11} \times S_{22} \times (\alpha_T^4 + \beta_T^4) \\ & - S_{22}^2 (\alpha_T^2 - \beta_T^2)] \times \sin(\alpha_T L) \times \sinh(\beta_T L) \\ & + 2 \times [S_{11}^2 \beta_T^3 \times \alpha_T^3 + S_{11} \times S_{22} \\ & \times (\alpha_T^3 \times \beta_T - \alpha_T \times \beta_T^3) - S_{22}^2 (\alpha_T \times \beta_T)] \\ & \times (\cos(\alpha_T L) \times \cosh(\beta_T L) - 1) = 0 \end{aligned} \quad (54)$$

By substituting with α and β from Eq. (46) in the above determinant and solve it numerically to get the natural frequency ω .

3.2.3 Cantilever BCs

For this case, the boundary condition are: at $x = 0$; $W_0 = 0$, $\phi = 0$ at $x = L$; $M = V = 0$. Substitute with these conditions in Eqs. (46) and (47) leads to the following equations

$$c_2 + c_4 = 0 \quad (55a)$$

$$(-\alpha_T^3 S_{11} + \alpha_T S_{22}) c_1 + (\beta_T^3 S_{11} + \beta_T S_{22}) c_3 = 0 \quad (55b)$$

$$\begin{aligned} & \alpha_T^2 \sin(\alpha_T L) c_1 + \alpha_T^2 \cos(\alpha_T L) c_2 \\ & - \beta_T^2 \sinh(\beta_T L) c_3 - \beta_T^2 \cosh(\beta_T L) c_4 = 0 \end{aligned} \quad (55c)$$

$$\begin{aligned} & (-GA)_{eq} k_s S_{11} \alpha_T^2 + A_T \\ & + (GA)_{eq} k_s S_{22} \alpha_T [\cos(\alpha_T L) c_1 - \sin(\alpha_T L) c_2] \\ & + ((GA)_{eq} k_s S_{11} \beta_T^2 + A_T \\ & + (GA)_{eq} k_s S_{22}) \beta_T [\cosh(\beta_T L) c_3 + \sinh(\beta_T L) c_4] \\ & = 0 \end{aligned} \quad (55d)$$

By eliminating the coefficients c_3 and c_4 in the above system and setting the determinant of the coefficient matrix to zero, yields in

$$\begin{aligned}
 |K| = & A_T \times B_T \times \mu \times \alpha_T \times \beta_T^3 \\
 & - A_T \times B_T \times \mu \times \alpha_T^3 \times \beta_T \\
 & + 2 \times B_T \times C_T \times \mu^2 \times \alpha_T \times \beta_T \\
 & - A_T \times C_T \times \mu \times \alpha_T^3 \times \cos(\alpha_T L) \sinh(\beta_T L) \\
 & + A_T \times C_T \times \mu \times \beta_T^3 \times \cosh(\beta_T L) \sin(\alpha_T L) \\
 & - B_T \times C_T \times \mu^2 \times \alpha_T^2 \sin(\alpha_T L) \sinh(\beta_T L) \\
 & + B_T \times C_T \times \mu^2 \times \beta_T^2 \sin(\alpha_T L) \sinh(\beta_T L) \\
 & - 2A_T \times B_T \times \mu \times \alpha_T^2 \times \beta_T^2 \\
 & \times \sin(\alpha_T L) \sinh(\beta_T L) \\
 & - A_T \times B_T \times \mu \times \alpha_T \times \beta_T^3 \cos(\alpha_T L) \cosh(\beta_T L) \\
 & + A_T \times B_T \times \mu \times \alpha_T^3 \times \beta_T \cos(\alpha_T L) \cosh(\beta_T L) \\
 & - 2B \times C_T \times \mu^2 \times \alpha_T \times \beta_T \cos(\alpha_T L) \cosh(\beta_T L) \\
 & - A_T \times C_T \times \mu \times \alpha_T \times \beta_T^2 \cos(\alpha_T L) \sinh(\beta_T L) \\
 & + A_T \times C_T \times \mu \times \alpha_T^2 \times \beta_T \sin(\alpha_T L) \cosh(\beta_T L) = 0
 \end{aligned}$$

Substitute with α_T and β_T in the above determinant and solve it numerically to get the natural frequency ω .

3.2.4 Propped BCs

For a propped beam, the boundary condition are: at $x = 0$; $W_0 = 0$, $\phi = 0$ and at $x = L$; $W_0 = M = 0$. Substitute with these conditions in Eqs. (46) and (47) leads to the following relations

$$\begin{bmatrix} 0 & 1 & 0 & 1 \\ \alpha_T & 0 & \beta_T & 0 \\ \sin(\alpha_T L) & \cos(\alpha_T L) & \sinh(\beta_T L) & \cosh(\beta_T L) \\ A_T \alpha_T^2 \sin(\alpha_T L) & A_T \alpha_T^2 \cos(\alpha_T L) & -A_T \beta_T^2 (\sinh(\beta_T L)) & A_T \beta_T^2 \cosh(\beta_T L) \end{bmatrix} \begin{Bmatrix} c_1 \\ c_2 \\ c_3 \\ c_4 \end{Bmatrix} = \{0\} \quad (56)$$

By eliminating the coefficients c_3 and c_4 in the above system and setting the determinant of the coefficient matrix to zero, yields in

$$\begin{aligned}
 |K| = & -A_T(\alpha_T^2 + \beta_T^2) \times [(\beta_T^2 S_{11} + S_{22})\beta_T \\
 & \times \tan(\alpha_T L) + (\alpha_T^2 S_{11} - S_{22})\alpha_T \times \tanh(\beta_T L)] \\
 = & 0
 \end{aligned}$$

Since $A_T(\alpha_T^2 + \beta_T^2) \neq 0$, so: (52)

$$\begin{aligned}
 & [(\beta_T^2 S_{11} + S_{22})\beta_T \times \tan(\alpha_T L) \\
 & + (\alpha_T^2 S_{11} - S_{22})\alpha_T \times \tanh(\beta_T L)] = 0
 \end{aligned}$$

Yields, $(S_{22} - \alpha_T^2 S_{11})\alpha * \tanh(\beta_T L) = (\beta_T^2 S_{11} + S_{22})\beta_T * \tan(\alpha_T L)$

Substitute with α_T and β_T into Eq. (55) and solve it numerically to get the natural frequency ω .

4. Numerical results

Through this section, proposed model will be validated with the previous works, and parameter studies will be developed to illustrate effects of number of holes, filling ratio, size scale parameter, and shear deformation on natural frequencies of thin or thick perforated beams with different boundary conditions.

4.1 Model validation

The fundamental frequency of full Euler and Timoshenko nanobeam with the following characteristics

Table 1 Comparison of non-dimensional fundamental frequencies for TNNB and TKNB

Nonlocal parameter	Present		Reddy (2007)	
	TNNB	TKNB	TNNB	TKNB
0.0	9.8594	9.8281	9.8696	9.8381
1.0	9.4062	9.3762	9.4159	9.3858
2.0	9.0102	8.9815	9.0195	8.9907
3.0	8.6604	8.6327	8.6693	8.6416
4.0	8.3483	8.3217	8.3569	8.3302
5.0	8.0677	8.0421	8.0761	8.0503

$[E = 30 \times 10^6, \nu = 0.3, G = \frac{E}{2(1+\nu)}, \rho = 1, L = 10, b = h = \frac{L}{20}, k_s = \frac{5}{6}]$ are exploited in computing the numerical values. The non-dimensional frequency is calculated by using the following formula $\lambda_i = \omega_i L^2 \sqrt{\frac{m_0}{EI}}$. The present and Reddy (2007) results as illustrated and compared in Table 1. As shown, the frequency of nanobeam is decreased by increasing the nonlocal parameter for both TNNB and

TKNB. The frequency of TNNB is greater than the frequency of TKNB at the same nonlocal parameter, due to the presence of shear effect. As observed from Table 1, the current model is validated with previous work of Reddy, since no significant deviation is noticed.

4.2 Parametric studies

Through this section, effects of number of holes, filling ratio, and nanoscale parameter on the natural frequencies of clamped, cantilever, and propped perforated nanobeams are discussed. The analysis assumed that [110] single crystal silicon nanobeam with the following parameters

$$\begin{aligned}
 E = 169 \text{ GPa}, \quad \mu = 0.064, \quad G = 79.6 \text{ GPa}, \\
 \rho = 2.329e3 \text{ kg/m}^3, \quad \text{and} \quad k_s = 5/6.
 \end{aligned}$$

The beam has the following dimensions, length $L = 141.1 \text{ nm}$, width $b = 46.9 \text{ nm}$, and thickness $h = L/20$.

4.2.1 Effect of filling ratio

The effect of filling ratio on the fundamental frequency of perforated macro/nanobeams for clamped BCs is present in Fig. 2. As presented from figures, NEB and NTB are identical and have the same natural frequencies at full beam $\alpha = 1$. However, reducing the filling ratio less than one, the shear effect on natural frequencies become significant. The filling ratio has opposite effect on NEB vs NTB. As shown in case of NEB, as the filling ratio decreases the fundamental frequencies increases significantly. However, in case of NTB, the reducing of filling ration tends to

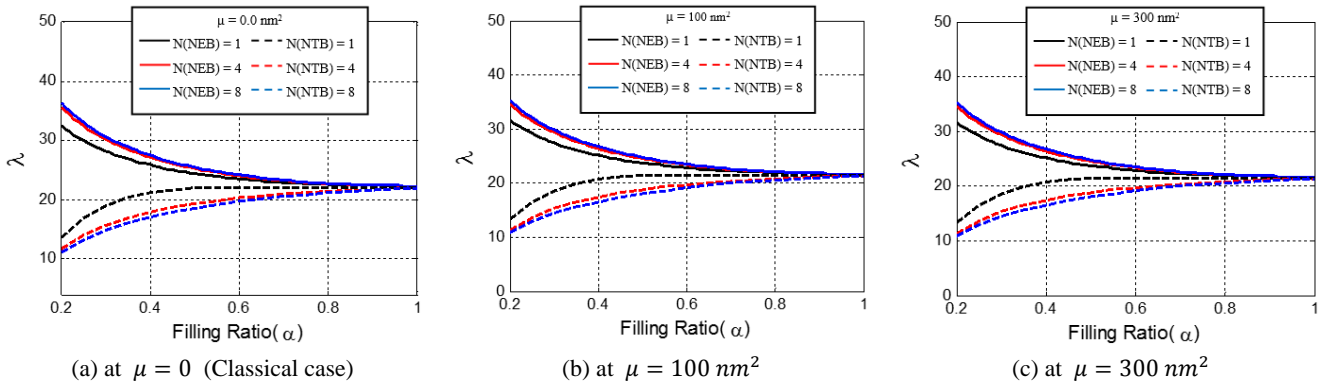


Fig. 2 Effect of filling ratio and number of holes along the section on fundamental frequencies for clamped BCs

decrease the fundamental frequencies. The filling ratio and shear effect are more significant within range of $(0.2 < \alpha < 0.9)$. It is not logic to calculate the natural frequency when $\alpha < 0.2$, because in this case, the beam is approximately fully empty.

Effects of filling ratio on the fundamental frequencies of cantilever and propped nanobeam are presented in Figs. 3 and 4, respectively. As shown, the filling ratio is most significant in the range of $(0.2 < \alpha < 0.8)$ in case of cantilever BCs, and $(0.2 < \alpha < 0.9)$ in case of propped beam. In these ranges, filling ratio tends to increase the natural frequencies as it increases in case of NTB. On the otherwise, by increasing the filling ratio, NEB fundamental

frequencies are decreased. It is noted that specially, at $\mu = 300 \text{ nm}^2$ for cantilever BCs, NEB is overestimated than NTB even that when $\alpha = 1$. For other all cases, NEB and NTB are identically for full beam without perforation.

4.2.2 Effect of number of holes

The effect of number of holes on the natural frequencies with varying the nanaoscale parameter, for a specified filling ratio and different boundary conditions are illustrated in Figs. 5-7. For a case in hand at smaller filling ratio ($\alpha = 0.2, 0.5$), the highest frequency observed for NEB at $N_E = 8$ and the smallest frequency noticed for NTB at $N_T = 8$. It is noticed, as the number of holes increase in case of NEB, the

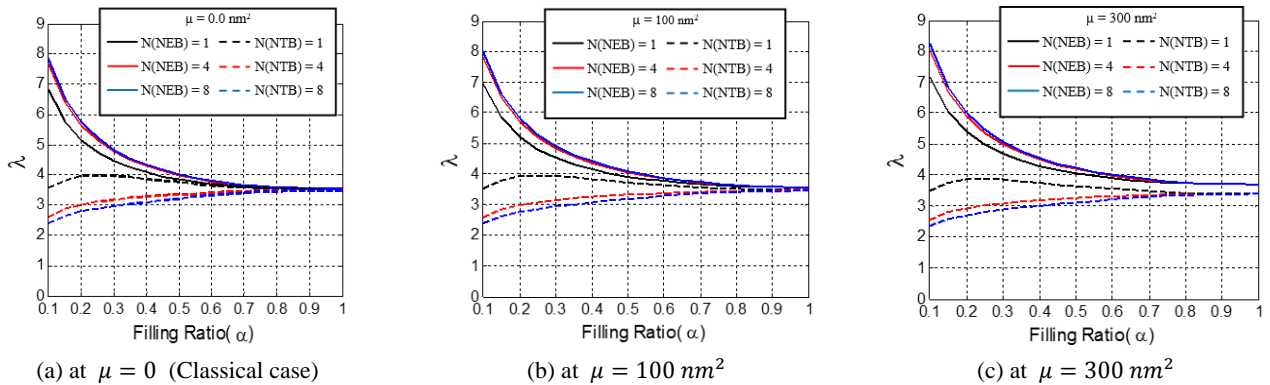


Fig. 3 Effect of filling ratio and number of holes along the section on fundamental frequencies for cantilever BCs

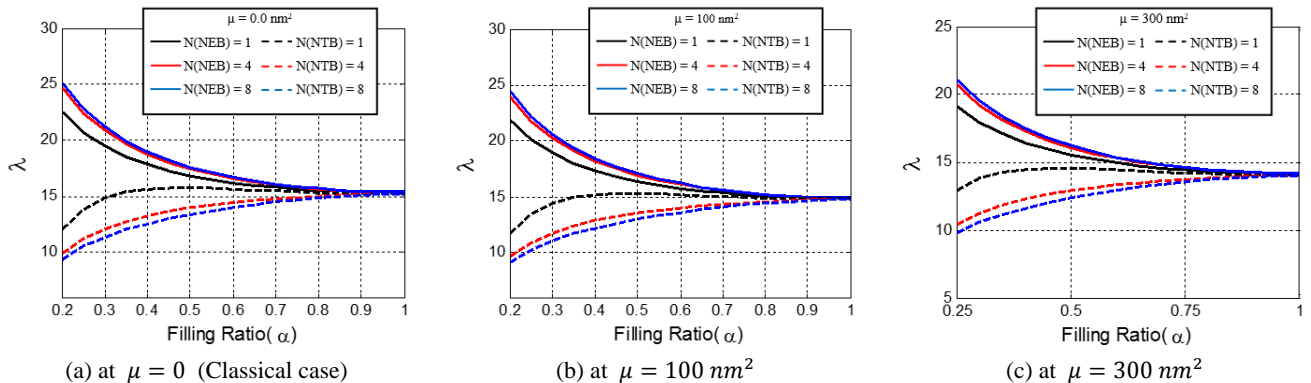


Fig. 4 Effect of filling ratio and number of holes along the section on fundamental frequencies for Propped BCs

natural frequency is increased. However, in case of NTB, as the number of holes increased, the natural frequency is decreased for all boundary conditions. As seen, increasing the hole number from 1 to 4 is more pronounced than increasing hole number from 4 to 8, for small filling ratio. In case of $\alpha = 0.9$, the hole number becomes insignificant on the natural frequencies for clamped, cantilever and propped beams. In case of clamped case at of $\alpha = 0.9$, the beam theory has not affected on the natural frequency as shown in Fig. 5(c), where the frequency of NEB and NTB are approximately identical. However, Beam theory has a significant influence on the natural frequency of cantilever and propped boundary conditions, where NEB is larger than

NTB at the same filling ratio, hole number, and nonlocal parameters.

4.2.3 Effect of nonlocal parameter

As shown from Figs. 5-7, as the nonlocal parameter increased, the natural frequency is decreased significantly due to the softening of the material. It is observed that, for clamped and propped boundary conditions, the natural frequency proportional inversely linear with the nonlocal parameter. However, in case of cantilever, the natural frequency proportional inversely nonlinear with nonlocal parameter. It is noticed that, the nonlocal parameter has the same effect on both NEB and NTB.

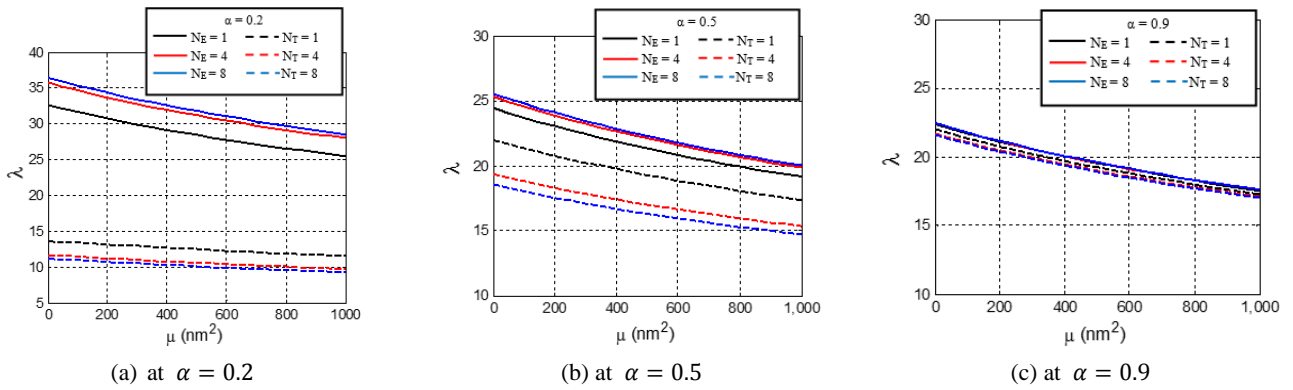


Fig. 5 Effect of number of holes with varying nonlocal parameter on fundamental frequencies for Clamped BCs

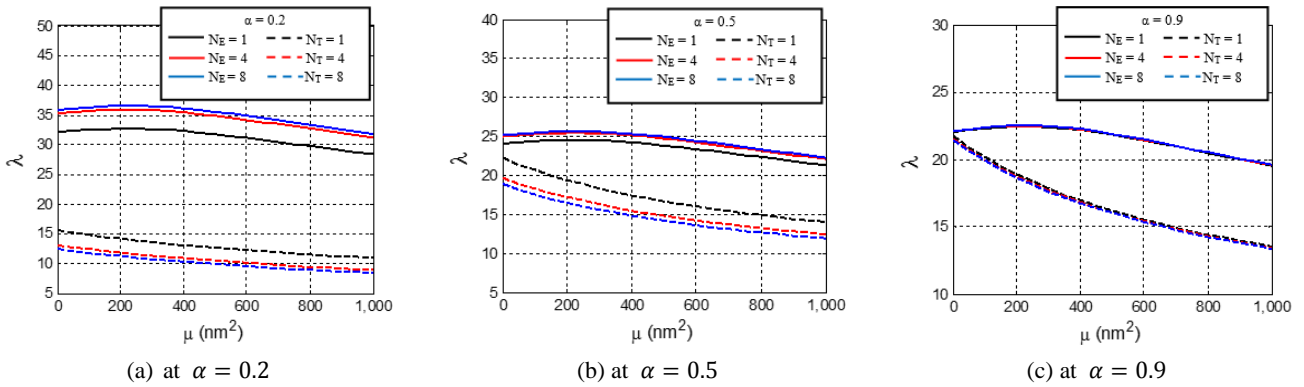


Fig. 6 Effect of number of holes with varying nonlocal parameter on fundamental frequencies for Cantilever BCs

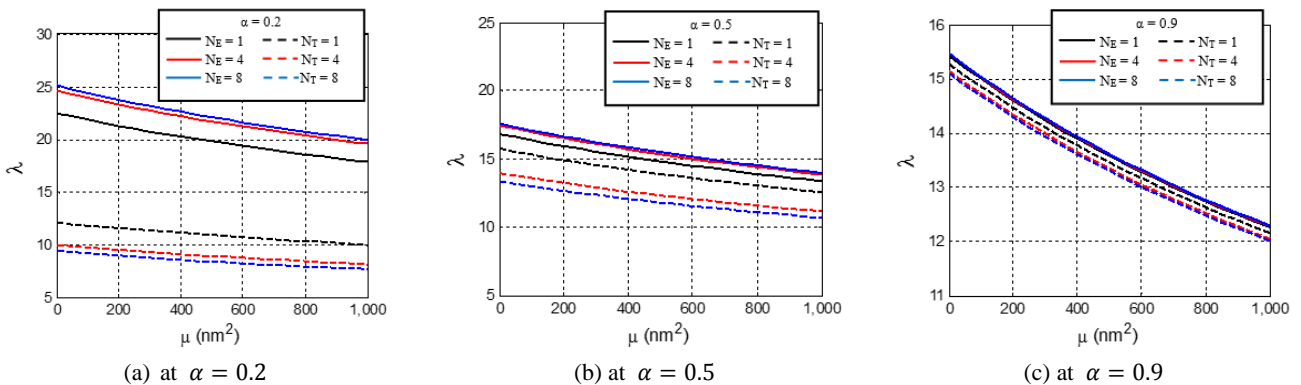


Fig. 7 Effect of number of holes with varying nonlocal parameter on fundamental frequencies for Propped BCs

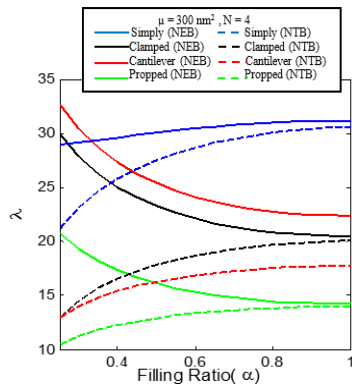


Fig. 8 Effect of filling ratio on the natural frequency at different boundary conditions

4.2.4 Effect boundary conditions

The effect of filling ratio and boundary conditions on the fundamental frequency at specified hole number and nonlocal parameter is presented in Fig. 8. As noticed for $\alpha > 0.4$, the highest natural frequency is observed in case of simply supported beam for both NEB and NTB, and the smallest natural frequency is noticed in case of propped boundary conditions for both NEB and NTB. It is observed frequencies of clamped and cantilever lay between simply and propped boundary conditions. Frequencies of clamped and cantilever boundary conditions can be arranged in the following descending order: - cantilever (NEN), clamped (NEB), clamped (NTB), and cantilever (NTB).

5. Conclusions

This investigation tries to complete the previous work of Eltahir (2018c), to consider the natural frequency of perforated nanobeam with different boundary conditions, that not studied elsewhere. The effect of long-range atomic interaction of nanobeam is adopted by nonlocal differential from of Eringen. The kinematic assumption of Euler-Bernoulli and Timoshenko beam theories are assumed to illustrate the shear effects on the vibrational phenomenon. Closed form and numerical solutions for natural frequency are derived in detail for all boundary conditions. Effects of boundary conditions, hole number, filling ratio and nanoscale parameter on the fundamental frequency are illustrated and discussed in detail. The main deductions resulting from the parametric studies can be summarized as:

- (1) The filling ratio is most significant in the range of ($0.2 < \alpha < 0.8$) in case of cantilever BCs, and ($0.2 < \alpha < 0.9$) in case of clamped and propped beams.
- (2) The filling ratio has opposite effect on NEB vs NTB.
- (3) At smaller filling ratio ($\alpha = 0.2, 0.5$), the highest frequency observed for NEB and $N_E = 8$ and the smallest frequency noticed for NTB and $N_T = 8$.
- (4) As the nonlocal parameter increased, the natural frequency is decreased significantly due to the softening of the material.

- (5) The highest natural frequency is observed in case of simply supported beam for both NEB and NTB, and the smallest natural frequency is noticed in case of Propped boundary conditions for both NEB and NTB.

Acknowledgments

This work was supported by the Deanship of Scientific Research (DSR), King Abdulaziz University, Jeddah, under Grant no. (DF-059-135-1441). The authors, therefore, gratefully acknowledge the DSR technical and financial support.

References

- Abdalrahmaan, A.A., Eltahir, M.A., Kabeel, A.M., Abdraboh, A.M. and Hendi, A.A. (2019), "Free and forced analysis of perforated beams", *Steel Compos. Struct., Int. J.*, **31**(5), 489-502. <https://doi.org/10.12989/scs.2019.31.5.489>
- Akbaş, Ş.D. (2016), "Forced vibration analysis of viscoelastic nanobeams embedded in an elastic medium", *Smart Struct. Syst., Int. J.*, **18**(6), 1125-1143. <https://doi.org/10.12989/sss.2016.18.6.1125>
- Akbaş, Ş.D. (2017a), "Free vibration of edge cracked functionally graded microscale beams based on the modified couple stress theory", *Int. J. Struct. Stabil. Dyn.*, **17**(3), 1750033. <https://doi.org/10.1142/S021945541750033X>
- Akbaş, Ş.D. (2017b), "Forced vibration analysis of functionally graded nanobeams", *Int. J. Appl. Mech.*, **9**(7), 1750100. <https://doi.org/10.1142/S1758825117501009>
- Akbaş, Ş.D. (2018a), "Forced vibration analysis of cracked nanobeams", *J. Brazil. Soc. Mech. Sci. Eng.*, **40**(8), 392. <https://doi.org/10.1007/s40430-018-1315-1>
- Akbaş, Ş.D. (2018b), "Forced vibration analysis of cracked functionally graded microbeams", *Adv. Nano Res., Int. J.*, **6**(1), 39-55. <https://doi.org/10.12989/anr.2018.6.1.039>
- Akbaş, Ş.D. (2018c), "Bending of a cracked functionally graded nanobeam", *Adv. Nano Res., Int. J.*, **6**(3), 219-242. <https://doi.org/10.12989/anr.2018.6.3.219>
- Akbaş, Ş.D. (2019), "Axially Forced Vibration Analysis of Cracked a Nanorod", *J. Computat. Appl. Mech.*, **50**(1), 63-68. <https://doi.org/10.22059/jcam.2019.281285.392>
- Almitani, K.H., Abdelrahman, A.A. and Eltahir, M.A. (2019), "On forced and free vibrations of cutout squared beams", *Steel Compos. Struct., Int. J.*, **32**(5), 643-655. <https://doi.org/10.12989/scs.2019.32.5.643>
- Apuzzo, A., Barretta, R., Luciano, R., de Sciarra, F.M. and Penna, R. (2017), "Free vibrations of Bernoulli-Euler nano-beams by the stress-driven nonlocal integral model", *Compos. Part B: Eng.*, **123**, 105-111. <https://doi.org/10.1016/j.compositesb.2017.03.057>
- Arani, A.G., Pourjamshidian, M., Arefi, M. and Arani, M. (2019), "Application of nonlocal elasticity theory on the wave propagation of flexoelectric functionally graded (FG) timoshenko nano-beams considering surface effects and residual surface stress", *Smart Struct. Syst., Int. J.*, **23**(2), 141-153. <https://doi.org/10.12989/sss.2019.23.2.141>
- Baroudi, S., Najar, F. and Jemai, A. (2018), "Static and dynamic analytical coupled field analysis of piezoelectric flexoelectric nanobeams: A strain gradient theory approach", *Int. J. Solids Struct.*, **135**, 110-124. <https://doi.org/10.1016/j.ijsolstr.2017.11.014>
- Barretta, R., Čanadija, M., Luciano, R. and de Sciarra, F.M. (2018), "Stress-driven modeling of nonlocal thermoelastic

- behavior of nanobeams”, *Int. J. Eng. Sci.*, **126**, 53-67.
<https://doi.org/10.1016/j.ijengsci.2018.02.012>
- Belmahi, S., Zidour, M., Meradjah, M., Bensattalah, T. and Dihaj, A. (2018), “Analysis of boundary conditions effects on vibration of nanobeam in a polymeric matrix”, *Struct. Eng. Mech., Int. J.*, **67**(5), 517-525. <https://doi.org/10.12989/sem.2018.67.5.517>
- Bourouina, H., Yahiaoui, R., Sahar, A. and Benamar, M.E.A. (2016), “Analytical modeling for the determination of nonlocal resonance frequencies of perforated nanobeams subjected to temperature-induced loads”, *Physica E*, **75**, 163-168.
<https://doi.org/10.1016/j.physe.2015.09.014>
- Chen, Y., Lee, J.D. and Eskandarian, A. (2004), “Atomistic viewpoint of the applicability of microcontinuum theories”, *Int. J. Solids Struct.*, **41**(8), 2085-2097.
<https://doi.org/10.1016/j.ijsolstr.2003.11.030>
- Cortés, C., Osorno, M., Uribe, D., Steeb, H., Ruiz-Salguero, O., Barandiarán, I. and Flórez, J. (2019), “Geometry simplification of open-cell porous materials for elastic deformation FEA”, *Eng. Comput.*, **35**(1), 257-276.
<https://doi.org/10.1007/s00366-018-0597-3>
- El-Sinawi, A.H., Bakri-Kassem, M., Landolsi, T. and Awad, O. (2015), “A novel comprehensive approach to feedback control of membrane displacement in radio frequency micro-electromechanical switches”, *Sensors Actuators A: Phys.*, **221**, 123-130. <https://doi.org/10.1016/j.sna.2014.11.004>
- Eltaher, M.A., Emam, S.A. and Mahmoud, F.F. (2012), “Free vibration analysis of functionally graded size-dependent nanobeams”, *Appl. Mathe. Comput.*, **218**(14), 7406-7420.
<https://doi.org/10.1016/j.amc.2011.12.090>
- Eltaher, M.A., Alshorbagy, A.E. and Mahmoud, F.F. (2013a), “Vibration analysis of Euler–Bernoulli nanobeams by using finite element method”, *Appl. Mathe. Model.*, **37**(7), 4787-4797.
<https://doi.org/10.1016/j.apm.2012.10.016>
- Eltaher, M.A., Alshorbagy, A.E. and Mahmoud, F.F. (2013b), “Determination of neutral axis position and its effect on natural frequencies of functionally graded macro/nanobeams”, *Compos. Struct.*, **99**, 193-201.
<https://doi.org/10.1016/j.compstruct.2012.11.039>
- Eltaher, M.A., Hamed, M.A., Sadoun, A.M. and Mansour, A. (2014), “Mechanical analysis of higher order gradient nanobeams”, *Appl. Mathe. Comput.*, **229**, 260-272.
<https://doi.org/10.1016/j.amc.2013.12.076>
- Eltaher, M.A., Khater, M.E. and Emam, S.A. (2016), “A review on nonlocal elastic models for bending, buckling, vibrations, and wave propagation of nanoscale beams”, *Appl. Mathe. Model.*, **40**(5), 4109-4128. <https://doi.org/10.1016/j.apm.2015.11.026>
- Eltaher, M.A., Fouda, N., El-midany, T. and Sadoun, A.M. (2018a), “Modified porosity model in analysis of functionally graded porous nanobeams”, *J. Brazil. Soc. Mech. Sci. Eng.*, **40**(3), 141. <https://doi.org/10.1007/s40430-018-1065-0>
- Eltaher, M.A., Kabeel, A.M., Almitani, K.H. and Abdraboh, A.M. (2018b), “Static bending and buckling of perforated nonlocal size-dependent nanobeams”, *Microsyst. Technol.*, **24**(12), 4881-4893. <https://doi.org/10.1007/s00542-018-3905-3>
- Eltaher, M.A., Abdraboh, A.M. and Almitani, K.H. (2018c), “Resonance frequencies of size dependent perforated nonlocal nanobeam”, *Microsyst. Technol.*, **24**, 3925-3937.
- Eltaher, M.A., Mohamed, N., Mohamed, S. and Seddek, L.F. (2019a), “Postbuckling of curved carbon nanotubes using energy equivalent model”, *J. Nano Res.*, **57**, 136-157.
<https://doi.org/10.4028/www.scientific.net/JNanoR.57.136>
- Eltaher, M.A., Almalki, T.A., Almitani, K.H. and Ahmed, K.I.E. (2019b), “Participation Factor and Vibration of Carbon Nanotube with Vacancies”, *J. Nano Res.*, **57**, 158-174.
<https://doi.org/10.4028/www.scientific.net/JNanoR.57.158>
- Eltaher, M.A., Omar, F.A., Abdraboh, A.M., Abdalla, W.S. and Alshorbagy, A.E. (2020a), “Mechanical behaviors of piezoelectric nonlocal nanobeam with cutouts”, *Smart Struct. Syst., Int. J.*, **25**(2), 219-228.
<https://doi.org/10.12989/sss.2020.25.2.219>
- Eltaher, M.A., Mohamed, S.A. and Melaibari, A. (2020b), “Static stability of a unified composite beams under varying axial loads”, *Thin-Wall. Struct.*, **147**, 106488.
<https://doi.org/10.1016/j.tws.2019.106488>
- Emam, S., Eltaher, M., Khater, M. and Abdalla, W. (2018), “Postbuckling and free vibration of multilayer imperfect nanobeams under a pre-stress load”, *Appl. Sci.*, **8**(11), 2238.
<https://doi.org/10.3390/app8112238>
- Eringen, A.C. (1972), “Nonlocal polar elastic continua”, *Int. J. Eng. Sci.*, **10**(1), 1-16.
[https://doi.org/10.1016/0020-7225\(72\)90070-5](https://doi.org/10.1016/0020-7225(72)90070-5)
- Eringen, A.C. (1983), “On differential equations of nonlocal elasticity and solutions of screw dislocation and surface waves”, *J. Appl. Phys.*, **54**(9), 4703-4710.
- Eringen, A.C. (2002), *Nonlocal Continuum Field Theories*, Springer Science & Business Media.
- Hamed, M., Sadoun, A.M. and Eltaher, M.A. (2019), “Effects of porosity models on static behavior of size dependent functionally graded beam”, *Struct. Eng. Mech., Int. J.*, **71**(1), 89-98.
<https://doi.org/10.12989/sem.2019.71.1.089>
- Hashemi, S.H. and Khaniki, H.B. (2018), “Dynamic response of multiple nanobeam system under a moving nanoparticle”, *Alexandria Eng. J.*, **57**(1), 343-356.
<https://doi.org/10.1016/j.aej.2016.12.015>
- Huang, Z. (2012), “Nonlocal effects of longitudinal vibration in nanorod with internal long-range interactions”, *Int. J. Solids Struct.*, **49**(15-16), 2150-2154.
<https://doi.org/10.1016/j.ijsolstr.2012.04.020>
- Jeong, K.H. and Amabili, M. (2006), “Bending vibration of perforated beams in contact with a liquid”, *J. Sound Vib.*, **298**(1), 404-419. <https://doi.org/10.1016/j.jsv.2006.05.029>
- Joshi, A.Y., Sharma, S.C. and Harsha, S.P. (2011), “Zeptogram scale mass sensing using single walled carbon nanotube based biosensors”, *Sensors Actuators A: Phys.*, **168**(2), 275-280.
<https://doi.org/10.1016/j.sna.2011.04.031>
- Kaghazian, A., Hajnayeb, A. and Foruzande, H. (2017), “Free vibration analysis of a piezoelectric nanobeam using nonlocal elasticity theory”, *Struct. Eng. Mech., Int. J.*, **61**(5), 617-624.
<https://doi.org/10.12989/sem.2017.61.5.617>
- Kerid, R., Bourouina, H., Yahiaoui, R., Bounekhla, M. and Aissat, A. (2019), “Magnetic field effect on nonlocal resonance frequencies of structure-based filter with periodic square holes network”, *Physica E: Low-dimens. Syst. Nanostruct.*, **105**, 83-89.
<https://doi.org/10.1016/j.physe.2018.05.021>
- Khadem, S.E., Rasekh, M. and Toghraee, A. (2012), “Design and simulation of a carbon nanotube-based adjustable nano-electromechanical shock switch”, *Appl. Mathe. Model.*, **36**(6), 2329-2339. <https://doi.org/10.1016/j.apm.2011.08.029>
- Li, L., Tang, H. and Hu, Y. (2018), “The effect of thickness on the mechanics of nanobeams”, *Int. J. Eng. Sci.*, **123**, 81-91.
<https://doi.org/10.1016/j.ijengsci.2017.11.021>
- Luschi, L. and Pieri, F. (2012), “A simple analytical model for the resonance frequency of perforated beams”, *Procedia Eng.*, **47**, 1093-1096. <https://doi.org/10.1016/j.proeng.2012.09.341>
- Luschi, L. and Pieri, F. (2014), “An analytical model for the determination of resonance frequencies of perforated beams”, *J. Micromech. Microeng.*, **24**(5), 055004.
<https://doi.org/10.1088/0960-1317/24/5/055004>
- Luschi, L. and Pieri, F. (2016), “An analytical model for the resonance frequency of square perforated Lamé-mode resonators”, *Sensors Actuators B: Chem.*, **222**, 1233-1239.
<https://doi.org/10.1016/j.snb.2015.07.085>
- Mohite, S.S., Sonti, V.R. and Prapat, R. (2008), “A compact squeeze-film model including inertia, compressibility, and

- rarefaction effects for perforated 3-D MEMS structures”, *J. Microelectromech. Syst.*, **17**(3), 709-723.
<https://doi.org/10.1109/JMEMS.2008.921675>
- Mouffoki, A., Bedia, E.A., Houari, M.S.A., Tounsi, A. and Mahmoud, S.R. (2017), “Vibration analysis of nonlocal advanced nanobeams in hygro-thermal environment using a new two-unknown trigonometric shear deformation beam theory”, *Smart Struct. Syst., Int. J.*, **20**(3), 369-383.
<https://doi.org/10.12989/sss.2017.20.3.369>
- Nagase, T., Kawamura, J., Pahlovy, S.A. and Miyamoto, I. (2010), “Ion beam fabrication of natural single crystal diamond nano-tips for potential use in atomic force microscopy”, *Microelectron. Eng.*, **87**(5), 1494-1496.
<https://doi.org/10.1016/j.mee.2009.11.070>
- Reddy, J.N. (2007), “Nonlocal theories for bending, buckling and vibration of beams”, *Int. J. Eng. Sci.*, **45**(2-8), 288-307.
<https://doi.org/10.1016/j.ijengsci.2007.04.004>
- Shao, L. and Palaniapan, M. (2008), “Effect of etch holes on quality factor of bulk-mode micromechanical resonators”, *Electron. Lett.*, **44**(15), 938-939.
<https://doi.org/10.1049/el:20081320>
- Sharma, J.N. and Grover, D. (2011), “Thermoelastic vibrations in micro-/nano-scale beam resonators with voids”, *J. Sound Vib.*, **330**(12), 2964-2977. <https://doi.org/10.1016/j.jsv.2011.01.012>
- Shen, J.P., Li, C., Fan, X.L. and Jung, C.M. (2017), “Dynamics of silicon nanobeams with axial motion subjected to transverse and longitudinal loads considering nonlocal and surface effects”, *Smart Struct. Syst., Int. J.*, **19**(1), 105-113.
<https://doi.org/10.12989/sss.2017.19.1.105>
- Simsek, M. (2019), “Some closed-form solutions for static, buckling, free and forced vibration of functionally graded (FG) nanobeams using nonlocal strain gradient theory”, *Compos. Struct.*, 111041. <https://doi.org/10.1016/j.compstruct.2019.111041>
- Tu, C. and Lee, J.E.Y. (2012), “Increased dissipation from distributed etch holes in a lateral breathing mode silicon micromechanical resonator”, *Appl. Phys. Lett.*, **101**(2), 023504.
<https://doi.org/10.1063/1.4733728>
- Zulkefli, M.A., Mohamed, M.A., Siow, K.S., Majlis, B.Y., Kulothungan, J., Muruganathan, M. and Mizuta, H. (2018), “Stress analysis of perforated graphene nano-electro-mechanical (NEM) contact switches by 3D finite element simulation”, *Microsyst. Technol.*, **24**(2), 1179-1187.
<https://doi.org/10.1007/s00542-017-3483-9>